

## Study of Time Evolution of Toroidal current in LHD

WATANABE Kiyomasa, SAKAKIBARA Satoru, SASAO Hajime<sup>1</sup>, YAKOVLEV Michael,  
NISHIMURA Kiyohiko, MURAKAMI Sadayoshi, NAKAJIMA Noriyoshi, YAMADA Hiroshi,  
NARIHARA Kazushige, YAMADA Ichihiko, TANAKA Kenji, KAWAHATA Kazuo,  
TOKUZAWA Tokihiko, IDA Katsumi, MORITA Shigeru, KANEKO Osamu, TSUMORI Katsuyoshi,  
IKEDA Katsunori, NARUSHIMA Yoshirou, MORISAKI Tomohiro, KOMORI Akio,  
LHD experimental group and LHD device engineering group

*National Institute for Fusion Science, Toki, Gifu 509-5292, Japan*

<sup>1</sup> *Japan Atomic Energy Research Institute, Ibaragi, 311-0193, Japan*

(Received: 21 December 2001 / Accepted: 18 June 2002)

### Abstract

We study the properties of non-inductive current in LHD experiments. The experimentally observed dependence on the plasma stored energy and the magnetic axis position agrees with a theoretical prediction based on bootstrap current under NB balanced injection. We apply a calculation model of time evolution in toroidal current profile based on bootstrap current and Ohkawa current to analyzing the dynamic change of the rotational transform in a discharge with fairly high beta and high positive toroidal current. The numerical analysis suggests that the disappearance of  $t=1/2$  rational surface leads to the sudden disappearance of the  $m/n=2/1$  magnetic fluctuation experimentally observed.

### Keywords:

bootstrap current, Ohkawa current, neutral beam, heliotron, LHD, MHD stability

### 1. Introduction

In helical devices, net toroidal current is not necessary to produce the magnetic field for plasma confinement. Over 100kA of net toroidal current has been observed in NBI plasmas of LHD (a device of heliotron) [1]. In typical LHD experiments, we do not drive ohmic current actively. Bootstrap current and Ohkawa current are theoretically considered as the candidates of the non-inductive current source. The observed toroidal current is not large enough to activate current driven instabilities. However, there is a possibility that it affects the MHD stability and transport through changing of the magnetic configurations [2,3]. The toroidal current with the direction to increase the rotational transform, which we call co-direction or positive, leads to the decrease in the magnetic shear and

the suppression of Shafranov shift which restrains the formation of magnetic well. The above effect is more sensitive on the current profile than the net current. In helical systems, the direct measurement of toroidal current profile is difficult because the additional change of the poloidal field to the vacuum field should be detected. Then it is important to identify the driving mechanism of the toroidal current, which leads to the construction of the reasonable model for the determination of current profile in present experiments as well as in reactor designs.

In the typical LHD-NBI discharge, the duration time of heating plasma is less than 5s. On the contrary, the relaxation time of the toroidal current is over 9s for the plasma with 3 keV as the central electron

*Corresponding author's e-mail: kiyowata@LHD.nifs.ac.jp*

©2002 by The Japan Society of Plasma  
Science and Nuclear Fusion Research

temperature, which we have obtained in LHD experiments [4]. Then it is necessary to analyze the time evolution of net toroidal current in order to estimate non-inductive current. In LHD device, the coil power supply is controlled to keep coil currents constant even while the plasma exists. However, the response time of the control is over 10s. As the results, any feedback control of the coil current is not effective during a typical plasma discharge, and the helical coil currents and poloidal coil currents change during the plasma discharge, which might affect to the estimation of the non-inductive currents. In this paper, we analyze the time evolution of toroidal current taking the mutual coupling due to coil currents into account. The properties of the non-inductive current are studied in balanced NB injected plasma.

In LHD experiments with fairly high beta and high positive toroidal current, the  $m/n=2/1$  magnetic fluctuation mode, which is observed from the initial phase, disappears suddenly as the beta and the net toroidal current increase [5]. The most probable explanation is the disappearance of  $t=1/2$  rational surface in the plasma region due to the fairly high beta and high positive toroidal current. In order to identify the current driven mechanism in LHD experiments, we apply a calculation model of time evolution in toroidal current profile based on bootstrap current and Ohkawa current to analyzing the dynamic change of rotational transform in the above-mentioned discharge.

This paper is organized as follows: in Sec. 2, we show the experimental setup and the way to estimate the non-inductive current. The properties of the non-inductive current under NB balanced injection are shown, and the comparison between the experimental results and the theoretical prediction is shown in Sec. 3. In Sec. 4, we show a calculation model of time evolution of toroidal current profile and result of its application. In Sec. 5, the results are summarized.

## 2. Experimental Setup

LHD is a heliotron device with  $L = 2$  and  $M = 10$  super-conducting helical coils and three pairs of poloidal coil [6]. Here  $L$  is a pole number and  $M$  is the field period of helical coil system. The device major radius is 3.9 m, and the plasma minor radius is 0.64 m in a typical operation. The net toroidal current and plasma-stored energy are measured with Rogowski coils and diamagnetic loops installed inside vacuum vessel, respectively. The eddy current in the helical coil can, and the summation of the eddy current in vacuum vessel

and supporting structures are measured with Rogowski coils. The current increment of the helical coils and poloidal coils are also measured. The magnetic fluctuation is measured with 64 three-axial magnetic probes along the helical coils, which are distributed at 6 toroidal locations. The electron density is obtained by the measurements with 13-channel far infrared laser interferometer. The electron temperature profile is measured with the multi-channel Thomson scattering system.

The non-inductive toroidal current,  $I_{NI}$ , is estimated by the following equation,

$$R_p I_p = V_{loop} + R_p I_{NI}. \quad (1)$$

Here  $I_p$  is the observed toroidal current and  $V_{loop}$  is the one turn voltage. In LHD, there is no loop coil to measure the one turn voltage inside the vacuum vessel. The one turn voltage is estimated by the following relationship in this paper,

$$V_{loop} = -L_p \frac{dI_p}{dt} + \sum_i M_{ip} \frac{dI_i}{dt}, \quad (2)$$

where the 1st term and the 2nd term in right hand side are the self-induced part and the mutual coupling parts, respectively.  $dI_i/dt$  is the current increment in components surrounding the plasma.  $i$  denotes a component surrounding the plasma such as helical coils, poloidal coils and so on.  $L_p$  and  $M_{ip}$  are the self-inductance of plasma and the mutual inductance between plasma and a component surrounding the plasma, respectively. In this paper, the following expressions are used as  $L_p$ , and  $R_p$ .

$$\begin{aligned} L_p &= L_{ext} + l_i, \quad L_{ext} = \mu_0 R \left( \log \frac{8R}{a} - 2 \right), \\ l_i &= \frac{1}{4} \mu_0 R, \quad R_p = 2\pi R \int \sigma dS, \\ \sigma &= \sigma_{spitz} (1 - \sqrt{\epsilon}) \left( 1 + 0.039\sqrt{\epsilon} \right) / \left( 1 + 0.471\sqrt{\epsilon} \right), \end{aligned}$$

where  $L_{ext}$  is the external self-inductance,  $l_i$  is the internal self-inductance,  $\sigma$  is the neoclassical electric conductivity,  $\sigma_{spitz}$  is so called Spitzer conductivity and  $\epsilon$  is the toroidal ripple of magnetic field strength. Here we adopt the equivalent tokamak's model as the neoclassical conductivity. The validity of the above assumption should be made clear in future. A calculated database based on multi-filament model is used as  $M_{ip}$ , which agrees with experimental results [7].

Figure 1 shows the time evolution of the observed toroidal current, the non-inductive current, the one turn voltage, the self-induced part and the mutual coupling parts in a NBI discharge. One turn voltage increases in the initial phase of discharge ( $t=0.5-1s$ ), and then

decreases. That reason is because the density rapidly increases in the initial phase, which leads to the increase of the non-inductive current (driven by NB here) and the resistivity. After  $t=1$ s, the density and the temperature are almost constant, the non-inductive current and the resistivity are also constant. One turn voltage decreases as the plasma current approaches to the non-inductive current. Here so-called  $L/R$  time is  $\sim 3.8$ s because the electron temperature keeps almost constant  $T_{e0} \sim 1.8$  keV. According to Fig. 1, the self-induced part of the one turn voltage is three times larger than the summation of the mutual coupling parts. In the present power supply control of the coil systems, the active control is not effective within 10s. Then the increment of the current in the components surrounding the plasma is induced by the increment of the toroidal plasma current, which leads to the mutual coupling part of one turn voltage in the typical discharge. In the steady state,  $dI_p/dt=0$ ,  $V_{loop}$  becomes almost 0. Here it should be noted that the inner helical coils contribution to one turn voltage is dominant among the mutual coupling parts.

We adopt the time averaged value of the non-inductive current, while the density and the electron temperature are almost constant, as the non-inductive current obtained experimentally. For example, the non-inductive current is averaged from  $t=1.5$ s to 3.0s in Fig. 1.

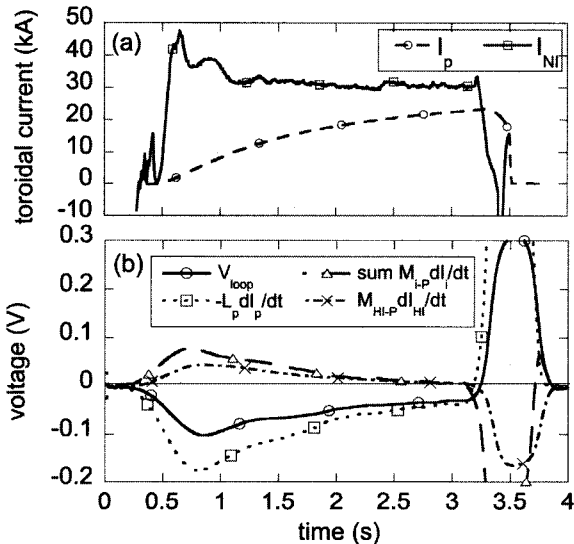


Fig. 1 Time evolution of the observed toroidal current,  $I_p$ , the estimated non-inductive current,  $I_{NI}$ , and the calculated one turn voltage,  $V_{loop}$ .

### 3. Non-Inductive Current Under Balanced NB Injection

In LHD balanced NBI discharges, we analyze the non-inductive current experimentally obtained from aspect of the dependence on the plasma stored energy and the magnetic axis position.

Figure 2 shows the dependence of the toroidal non-inductive current obtained experimentally on plasma-stored energy in NB balanced injected case. Here the ratio of differential port-through power between co and cntr. (counter) injected NB to total power is less than 7%. Then we can ignore Ohkawa current here. Magnetic axis is 3.75 m, operation magnetic field strength is 1.5 T and hydrogen gas-puff is adopted. The closed triangles are experimentally obtained data, which is estimated based on eq. (1) as mentioned in Sec. 2. Here the collisionalities of data in Fig. 2 belong to so-call  $1/\nu$ -regime at  $\rho=0.8$ . The experimental data are proportional to plasma-stored energy. The open circles are the theoretical prediction using SPBSC code, which calculates bootstrap current consistent with 3-dimensional MHD equilibrium [8]. In the calculation, the measurement data is used as the line averaged electron density,  $n_{e-bar}$  and the electron temperature,  $T_e$ , but  $n_e$  profile is assumed as  $\sim (1-\rho^8)$ .  $Z_{eff}=2$  and  $T_e=T_i$  are also assumed. The magnitude and direction of the observed plasma current fairly agree with the prediction of bootstrap current.

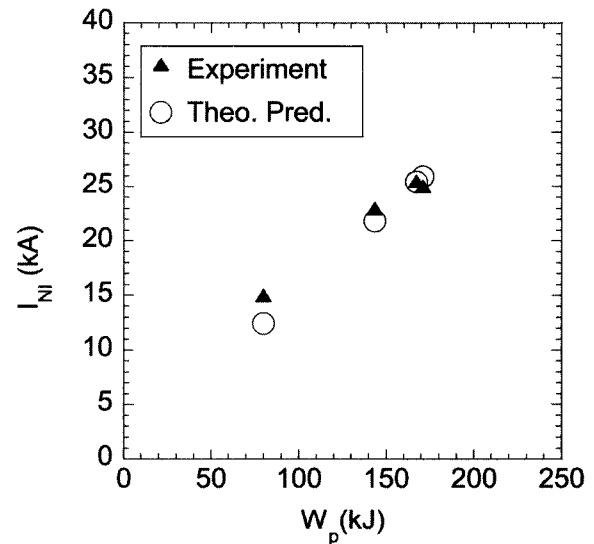


Fig. 2 The plasma stored energy dependence of the non-inductive current obtained experimentally, and the comparison between experimental results and the theoretical prediction.

Figure 3 shows the dependence of non-inductive current obtained experimentally on the magnetic configurations with different magnetic axis. The beta values are almost same,  $\langle\beta_{\text{dia}}\rangle=0.33\text{--}0.41\%$ . Here  $\langle\beta_{\text{dia}}\rangle$  is the volume averaged beta value. The data are obtained under a same condition of NB injection; co NB has port through power of 2 MW with beam energy of 150 keV, and two cntr. NBs have 0.6 MW with 120 keV and 1 MW with 150 keV, respectively. Circles denote the experimental data and a line denotes the theoretical prediction of bootstrap current by SPBSC code. We find that the experimentally obtained non-inductive current decreases as the magnetic axis goes torus-outwardly. The theoretical prediction also shows that the bootstrap current decreases with the torus-outward shift of the magnetic axis. That reason is because the magnetic configuration approaches to a poloidal symmetry system due to the torus-outward shift of the magnetic axis in LHD [2]. It should be noted that co beam current is a little superior to cntr. beam current as the above mentioned. According to a theoretical prediction by MCNBH code [9], which is based on 3-dimensional Monte Carlo simulation, the non-inductive current driven by the beam is approximately +5 kA. The effect of the unbalanced beam is not large here.

From the properties of the observed non-inductive current as shown in this section, the bootstrap current is

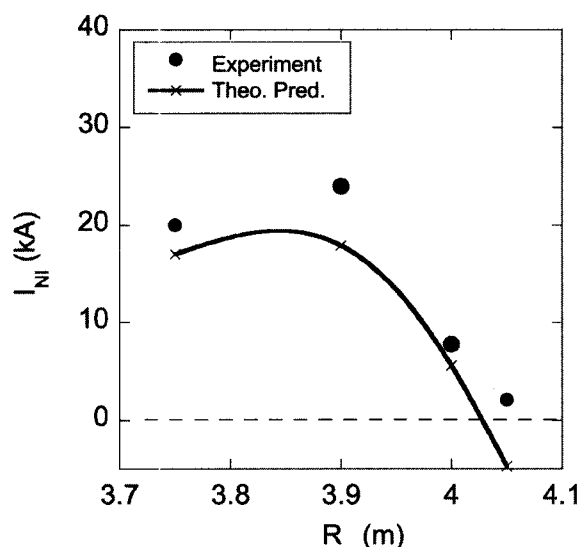


Fig. 3 The magnetic axis position dependence of the non-inductive current obtained experimentally under almost same beta, and the comparison between experimental results and the theoretical prediction.

the most probable candidate as the driving mechanism of non-inductive current in LHD experiments under balanced NB-injection.

#### 4. MHD Activity and Central Rotational Transform

In LHD experiments with " $R_{\text{ax}}=3.6$  m (magnetic axis torus-inwardly shifted) configuration", the  $m/n=2/1$  mode of magnetic fluctuation is observed generally in the range of the beta,  $\langle\beta_{\text{dia}}\rangle=0.3\text{--}2.3\%$  with the low toroidal current. The strong relationship between the observation of the  $m/n=2/1$  magnetic fluctuation and Mercier unstable condition is observed [5,10]. Here  $m$  and  $n$  are the poloidal and toroidal mode number, respectively. However, in experiments with fairly high beta and high positive toroidal current, the  $m/n=2/1$  mode observed by the magnetic probes from the initial phase disappears suddenly as the beta and the net toroidal current increase [5].

In Fig. 4, we show an example of the waveform of discharge, where the above event occurs. Co NB starts

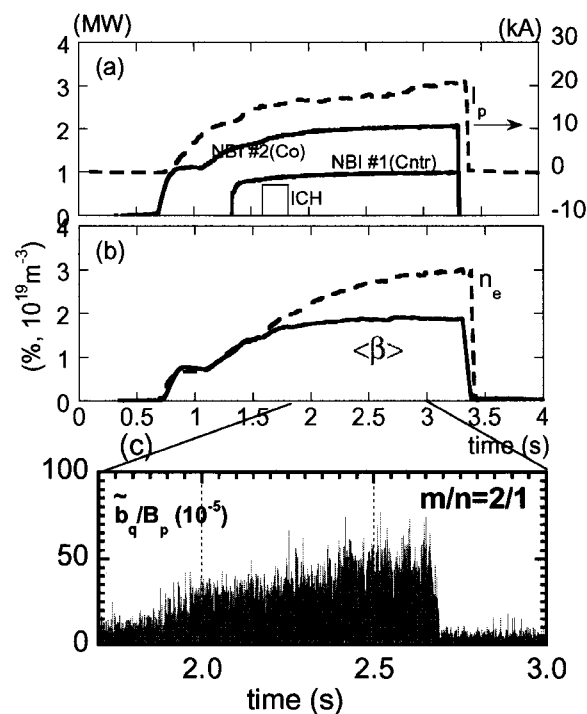


Fig. 4 Time trace of (a) deposited heating power and the toroidal plasma current, (b) the volume averaged beta and the line averaged electron density and (c) the amplitude of  $m/n=2/1$  magnetic fluctuation in the discharge, where the disappearance of the  $m/n=2/1$  mode occurs.

the injection earlier than cntr. NB, and the power of co NB is larger than cntr. NB, which leads to large positive toroidal current. The  $m/n=2/1$  mode has the frequency of about 1kHz, and it starts to increase at  $t=1.85$ s, and it disappears at  $t=2.66$ s. The other modes of magnetic fluctuation, for example, the  $m/n=2/2$  and  $2/3$  are observed both before and after the disappearance of the  $m/n=2/1$  mode. When the  $m/n=2/1$  mode disappears, the beta is around 1.8% and plasma current is around 18kA, which corresponds to 0.05 as the increment of  $t$  at the edge. Before and after the disappearance of the  $m/n=2/1$  mode, the beta and the plasma current gradually increases. Figure 5 shows the time trace of Mercier parameter,  $D_1$ , at the  $t=1/2$  rational surface, which is calculated with the pressure profile measured experimentally and under the net toroidal currentless assumption. According to currentless analysis,  $D_1$  at  $t=1/2$  rational surface is positive from  $t=1.5$ s to 3.0s, where Mercier modes are expected unstable.  $D_1$  after the disappearance of the  $m/n=2/1$  mode is larger than that before the disappearance. The above result and the strong relationship between the magnetic fluctuation and the Mercier condition show the possibility that the toroidal current stabilizes the  $m/n=2/1$  MHD unstable mode. Then the most probable candidate of the reason is the disappearance of the resonant rational surface,  $t=1/2$ , due to the toroidal current. When we assume that the disappearance of the magnetic fluctuation is due to the disappearance of the resonant rational surface, we can check the validity of the calculation model of the toroidal current profile evolution through the comparison between the dynamic change of rotational transform theoretically calculated and the timing of the appearance and/or the disappearance of the observed magnetic fluctuation.

The time evolution of the toroidal current is calculated by the following diffusion equation.

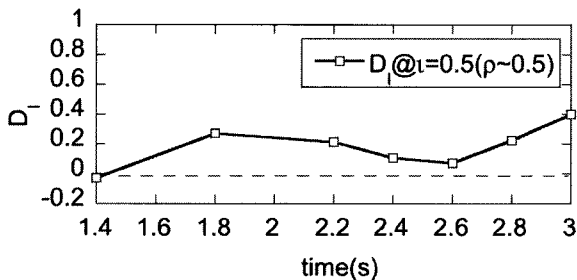


Fig. 5 Time trace of Mercier parameter under currentless assumption.

$$\mu_0 \frac{\partial I_p}{\partial t} = 4\pi S \frac{\partial}{\partial S} \left[ \frac{1}{\sigma} \frac{\partial}{\partial S} (I_p - I_{NI}) \right], \quad (3)$$

where  $I_p=I_p(S,t)$  and  $I_{NI}=I_{NI}(S,t)$  are the toroidal current and the non-inductive current inside a magnetic surface, and  $S$  is the toroidally averaged area enclosed by a magnetic surface,  $S=\pi r^2$ .  $r$  is the plasma minor radius. As the boundary condition, we apply the followings,

$$I_p(0, t) = 0, \quad (5)$$

$$\begin{aligned} & \frac{\partial}{\partial S} (I_p - I_{NI}) \Big|_{S=\pi a^2} \\ &= \sigma \frac{1}{2\pi R_0} \left( -L_{\text{exp}} \frac{\partial I_p}{\partial t} \Big|_{S=\pi a^2} + \sum_r M_{rIP} \frac{dI_r}{dt} \right). \end{aligned} \quad (6)$$

As the initial condition, we adopt  $I_p(S,t)=I_{p0}(S)$ . Here we are considering bootstrap current and Ohkawa current as the non-inductive current. Bootstrap current and Ohkawa current are calculated with the measured density and temperature by SPBSC code and MCNBH code.

Figure 6 denotes the comparison of the time evolution of between the observed net toroidal current and the calculation results. The thin and thick lines denote the experimental data and the calculation data, respectively. Dashed line is the summation of the bootstrap current and Ohkawa current, the magnitude of which is expected in the steady state. After  $t=1$ s, the plasma stored energy and the electron density gradually increase, and the electron temperature keeps almost

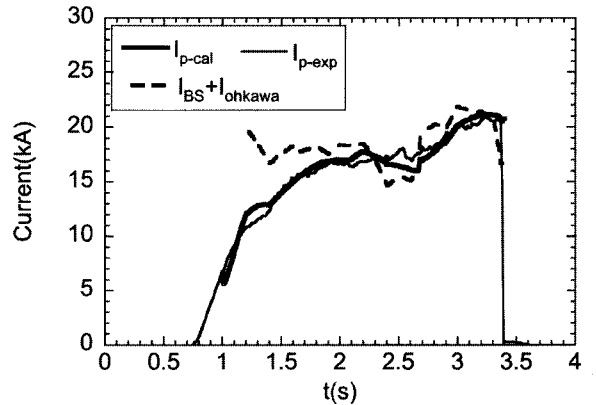


Fig. 6 Time evolution of the experimentally observed net toroidal current (thin line), the calculated plasma current (thick line) and the summation of the bootstrap current and Ohkawa current (dashed line).

constant. The summation of Ohkawa current and bootstrap current is almost constant after  $t=1.0$ s. That reason is because Ohkawa current is decreasing with the density increasing. On the contrary, the bootstrap current is increasing with the plasma stored energy increasing. From  $t=2.2$ s to 2.7s, the summation of bootstrap current and Ohkawa current is smaller than before  $t=2.2$ s because the bootstrap current is decreasing due to flat profile of central electron temperature. After  $t=2.7$ s, the electron temperature profile becomes peaked, which leads to the increase of bootstrap current and its more peaked profile. The time evolution of the calculated net plasma current fairly agrees with the experimental data. The evolution of plasma current density calculated with the diffusion equation, eq. (3), is shown in Fig. 7. The calculated plasma current profile

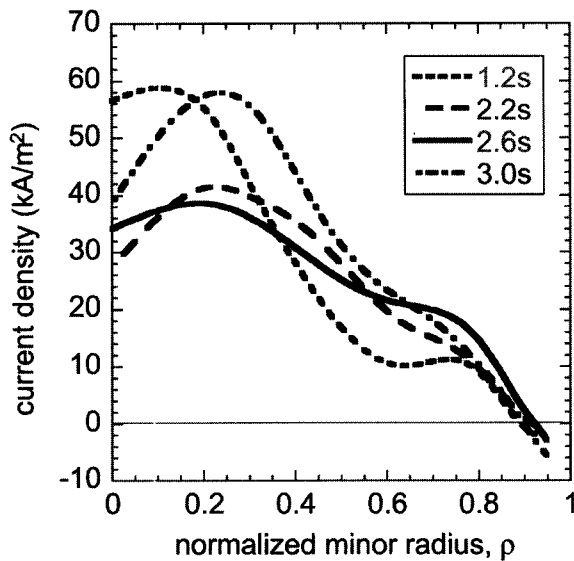


Fig. 7 Time evolution of calculated toroidal current density.

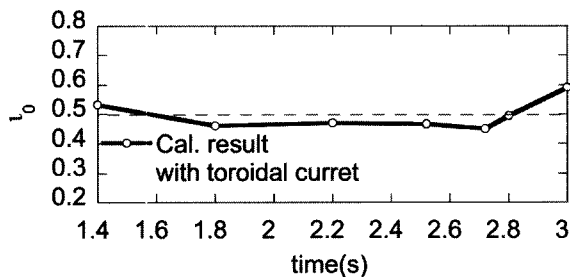


Fig. 8 Time trace of the central rotational transform with the calculated toroidal current based on the time evolution solving.

changes as the followings; peaked, flat and peaked again with changing of bootstrap current and Ohkawa current. Here  $L/R$  time due to the external inductance is around 0.9s and that  $L/R$  time due to the internal inductance is around 0.1s, which is corresponding to the relaxation time of current profile. Figure 8 shows the time trace of the central rotational transform. Before  $t=1.8$ s, the  $t=1/2$  rational surface is expected not to be in plasma region because the current profile is peaked. From  $t=1.8$ s to 2.7s, the  $t=1/2$  rational surface is expected to be in plasma region because the current profile becomes flat. After  $t=2.8$ s, the  $t=1/2$  rational surface is expected not to be in plasma region again because the current profile becomes peaked. From results of Fig. 4(c) and Fig. 8, the timing of the disappearance of the  $m/n=2/1$  magnetic fluctuation observed experimentally fairly agrees with the timing when the  $t=1/2$  rational surface theoretically estimated disappears.

## 5. Summary

In order to identify the toroidal current driving mechanism, the time evolution of the net toroidal current and its profile are analyzed for LHD plasmas.

We estimate the non-inductive current taking the mutual coupling due to the structure surrounding the plasma, such as coils, vacuum vessel and so on, into account. We study the properties of the non-inductive toroidal current and find that the bootstrap current is the most probable candidate as the driving mechanism of non-inductive current in LHD experiments under balanced NB injection. The study of non-inductive current in discharges under unbalanced NB injection is a future subject.

We analyze the time evolution of toroidal current profile in a fairly high beta LHD experiment with high toroidal current, where the sudden disappearance of the  $m/n=2/1$  magnetic fluctuation is observed, by using a calculation model based on bootstrap current and Ohkawa current. The timing of the disappearance of the  $m/n=2/1$  magnetic fluctuation fairly agrees with the timing when  $t=1/2$  rational surface theoretically estimated disappears. We find that the calculation model of the toroidal current profile proposed in this paper is quite helpful to the determination of toroidal current profile in a LHD experiment. Our goal is to establish the general calculation model of the toroidal current profile in LHD experiments. We should improve the calculation model through checking the validity of neoclassical conductivity, the estimation method of the one turn voltage and so on.

### References

- [1] K.Y. Watanabe *et al.*, in Controlled Fusion and Plasma Physics (Proc. 27th Eur. Conf. Budapest, 2000), **24B**, 1316 (2000).
- [2] K.Y. Watanabe *et al.*, Nucl. Fusion **41**, 63 (2001).
- [3] K. Ichiguchi *et al.*, Nucl. Fusion **33**, 481 (1993).
- [4] H. Yamada *et al.*, Plasma Phys. Control. Fusion **43**, A45 (2001).
- [5] S. Sakakibara *et al.*, Nucl. Fusion **41**, 1177 (2001).
- [6] A. Iiyoshi *et al.*, Nucl. Fusion **39**, 1245 (1999).
- [7] H. Chikaraishi *et al.*, in Proc. Int. Power Elec. Conf., Tokyo, (IPEC-2000), 1587 (2000).
- [8] K.Y. Watanabe *et al.*, Nucl. Fusion **35**, 335 (1995).
- [9] S. Murakami *et al.*, Trans. Fusion Technol. **27**, 259 (1995).
- [10] S. Sakakibara *et al.*, Plasma Phys. Control. Fusion **44**, A217 (2002).